

# Fe<sub>3</sub>O<sub>4</sub>@SiO<sub>2</sub> supported vanillin/Indole-sulfonic acid as a green, sustainable and magnetically reusable catalyst for the synthesis of mono-, bis- and tris- azo acridines

Leila Zare Fekri<sup>1,\*</sup> , Atefeh Alijani<sup>1</sup>, Mohammad Nikpassand<sup>2</sup>, Zahra Mohammadi<sup>1</sup>

<sup>1</sup>Department of Chemistry, Payame Noor University, PO Box 19395-3697 Tehran, Iran.

<sup>2</sup>Department of Chemistry, Ra.C., Islamic Azad University, Rasht, Iran.

\*Corresponding author: [leilazarefekri@pnu.ac.ir](mailto:leilazarefekri@pnu.ac.ir), [chem\\_zare@yahoo.com](mailto:chem_zare@yahoo.com)

## Original Research

Received:  
7 February 2025  
Revised:  
28 April 2025  
Accepted:  
17 May 2025  
Published online:  
28 May 2025

© 2025 The Author(s). Published by the OICC Press under the terms of the Creative Commons Attribution License, which permits use, distribution and reproduction in any medium, provided the original work is properly cited.

## Abstract:

Fe<sub>3</sub>O<sub>4</sub>@SiO<sub>2</sub> supported vanillin/Indole-sulfonic acid (Fe<sub>3</sub>O<sub>4</sub>@SiO<sub>2</sub>Pr@Vanillin@Indole-sulfonic acid) nanoparticles were synthesized and were characterized by FE-SEM, FT-IR, XRD, VSM, TEM, EDX, and TGA-DTG. Then, the application of this new nano catalyst for the multicomponent synthesis of azo-derived dihydropyridines via the reaction of azo-linked aldehydes, dimedone, and ammonium acetate was investigated. The procedure was carried out in high yields and short reaction times. Easy preparation of the catalyst and easy work-up are the main advantages of the protocol. The nanocatalyst can be reused for six reaction cycles with no notable decrease in catalytic efficiency. It is the first report to use Fe<sub>3</sub>O<sub>4</sub>@SiO<sub>2</sub>Pr@Vanillin@Indole-sulfonic acid for the synthesis of azoacridines. All of the organic compounds synthesized are new and were characterized carefully. The reaction times and yields for the synthesis of azoacridines are comparable to the reported methods for the synthesis of simple acridines. The reaction speed is suitable, and the productivity of this method is good. The reaction was carried out under solvent-free conditions and in green and mild conditions. The methodology described is completely new. The highlighted points of this work are as follows: 1) All of the synthesized azo-linked acridines are new. 2) The catalyst synthesized is completely new. 3) There is the first report for the synthesis of azo-linked dihydropyridines using Fe<sub>3</sub>O<sub>4</sub>@SiO<sub>2</sub> supported vanillin/Indole-sulfonic acid. 4) Shorter reaction times and higher yields, rather than most of the reported methods, are two major benefits of this work. 5) The reaction was carried out under solvent-free conditions, and there is no need to use organic and hazardous solvents in this procedure. 6) The reaction was carried out at room temperature, which requires no heating, and it is based on green chemistry rules because the method is energy-efficient.

**Keywords:** Azo-derived Dihydropyridines; Fe<sub>3</sub>O<sub>4</sub>@SiO<sub>2</sub>Pr@Vanillin@Indole-sulfonic acid; Green chemistry; Reusable catalyst; Solvent-free conditions

## 1. Introduction

1,4-Dihydropyridines were first synthesized by Arthur Hantsch in 1882 and have numerous biological properties such as antibacterial, antifungal, anti-Alzheimer, anti-diabetic, anti-atherosclerotic, vasodilator, and muscle relaxant [1–3]. In figure 1, some biologically active compounds, such as calcium channel blockers, were shown. Nifedipine was introduced in the early 1970s. After that, another calcium antagonist with more antihypertensive activity and better tissue selectivity was introduced. Felodipine, isradip-

ine, nicardipine (second generation), amlodipine, barnidipine, lercanidipine (third generation), and clinidipine (fourth generation) [4].

Arthur Hantsch synthesized 1,4-DHPs from the condensation of ethylacetoacetate, aldehyde, and ammonia in refluxing EtOH [5–7]. After the Hantsch method, various methods for the synthesis of DHPs were carried out. Some of them, are catalysts such as iodobenzene diacetate [8], Fe<sub>3</sub>O<sub>4</sub> nanoparticles [9], aluminum phosphate [10], melamine trisulfonic acid [11], gadolinium triflate [12], bis-

muth nitrate [13], mesoporous vanadium ion doped titania nanoparticles [14] and glycine nitrate (GlyNO<sub>3</sub>) ionic liquid [15].

Multicomponent reactions are procedures in which three or more components react together to synthesize a combined structure of all components. Multicomponent reactions have advantages such as breadth of molecular diversity, decreasing the reaction time, more effortless performance rather than multi-step syntheses, high efficiency of the reaction, being environmentally friendly, and a one-step procedure [16].

Magnetic nanoparticles have attracted a lot of interest because of their unique properties in various fields such as drug delivery [17], solar cells [18], biological labeling [19], heterogeneous catalysis [20], magnetic resonance imaging (MRI) [21], magnetic separations [22] and tissue engineering. It has superparamagnetic properties, a higher surface-to-volume ratio, and high biocompatibility. Fe<sub>3</sub>O<sub>4</sub> MNPs have advantages due to their high surface area, easy synthesis and handling, simple recoverability, oxidative stability, and nontoxicity. For these reasons, they are important in organic transformations. Fe<sub>3</sub>O<sub>4</sub> nanoparticles are oxidized in the air, so the nanoparticles are protected by a modifier against oxidation. They can be readily removed from the reaction vessel by an external magnetic field and are reusable [23–31].

As mentioned, there are a lot of avenues and methods for

the synthesis of DHPs [32]. However, there are some defects to these methods, such as being very expensive, toxic, and difficult to separate, clean, and recycle, which makes them difficult to use. Tedious workup procedures, being time-consuming, insufficient yields, requiring intense heat, and using risky solvents are other defects of reported methods. Therefore, the design and production of new catalytic alternates, which are active and stable, easily separable, and reusable, are highly interesting to use in organic reactions. On the other hands, synthesis of new derivatives of DHPs based on their essential biologically properties and evaluation of their biological activity such as anti-bacterial properties are of interest.

## 2. Experimental

### 2.1 General procedure and materials

We bought all the chemicals from Fluka and Merck. Melting points were determined by an Electrothermal 9100, and the data are accurate. <sup>1</sup>H NMR and <sup>13</sup>C NMR spectra were recorded in CDCl<sub>3</sub> on a Bruker DRX Advance instrument spectrometer using TMS as internal standard. IR spectra were obtained with an FT-IR 8600 with KBr pellets. XRD spectra were taken using a Bruker AXS (D8 Advance) X-ray diffractometer with Cu K $\alpha$  radiation ( $\lambda = 0.15418$  nm). The TESCAN Vega model instrument was used to take energy-dispersive spectroscopy (EDS).

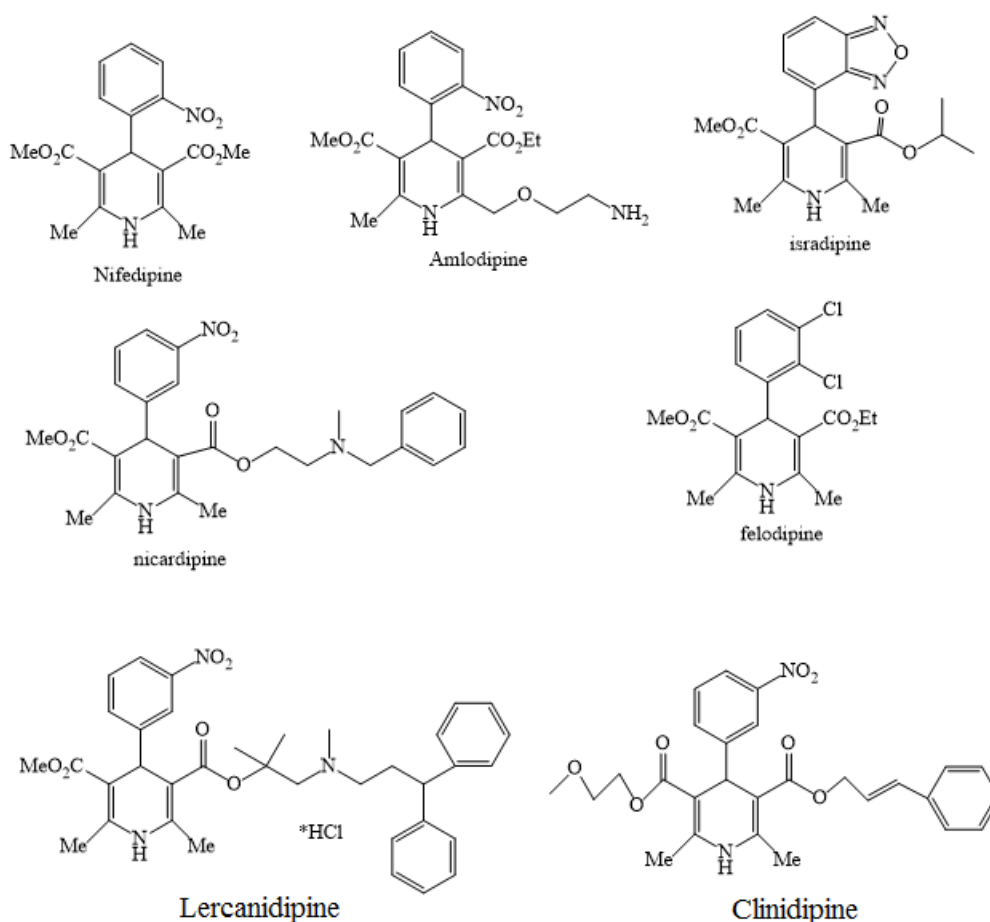


Figure 1. Some biologically active 1,4-DHPs.

## 2.2 Preparation of Fe<sub>3</sub>O<sub>4</sub> and Fe<sub>3</sub>O<sub>4</sub>@SiO<sub>2</sub>-prFe<sub>3</sub>O<sub>4</sub> and Fe<sub>3</sub>O<sub>4</sub>@SiO<sub>2</sub>-Pr

Preparation of Fe<sub>3</sub>O<sub>4</sub> and Fe<sub>3</sub>O<sub>4</sub>@SiO<sub>2</sub>-prFe<sub>3</sub>O<sub>4</sub> and Fe<sub>3</sub>O<sub>4</sub>@SiO<sub>2</sub>-Pr were prepared via the reported methods by Zare Fekri et al. [33, 34]

## 2.3 Fe<sub>3</sub>O<sub>4</sub>@SiO<sub>2</sub>-pr@vanilline

0.5 g of Fe<sub>3</sub>O<sub>4</sub>@SiO<sub>2</sub>-Pr NPs was stirred with 1.0 g of vanillin in the presence of 0.1 g sodium bicarbonate in 10 mL of EtOH for 24 hours. After completion of reaction, the reaction mixture was filtered and the NPs was separated and dried for 12 h.

## 2.4 Preparation of Fe<sub>3</sub>O<sub>4</sub>@SiO<sub>2</sub>-pr@vanilline/Indole

A mixture of 0.5 g of Fe<sub>3</sub>O<sub>4</sub>@SiO<sub>2</sub>-pr@vanilline and 1.2 g of indole were refluxed in the presence of 10 drops of acetic acid in 10 mL of EtOH. After 1 hour, the reaction mixture was filtered, and the catalyst was dried and used for the next step.

## 2.5 Preparation of Fe<sub>3</sub>O<sub>4</sub>@SiO<sub>2</sub>-pr@vanilline/Indole sulfonic acid

0.3 mL of chlorosulfonic acid was added dropwise to the mixture of 0.5 g of Fe<sub>3</sub>O<sub>4</sub>@SiO<sub>2</sub>-pr@vanilline/Indole in 10 mL of n-hexane in an ice/NaCl bath at 0 °C for 4h. Then the mixture was stirred for 8 h. The reaction mixture was filtered, and the catalyst was dried and used.

## 2.6 General procedure for the synthesis of azo-acridines

A mixture of 1 mmol of aldehyde, 2 mmol of dimedone, and one mmol of 4-aminoazobenzene was heated in the presence of 0.05 g of Fe<sub>3</sub>O<sub>4</sub>@SiO<sub>2</sub>-Pr@vanilline/Indole-SO<sub>3</sub>H at 80 °C. The reaction progress was monitored by TLC (4:1 n-hexane: EA). After completion of the reaction, 10 mL of EtOH was added to the mixture. The mixture was filtered in the presence of an enormous magnetic bar to separate the catalyst. The ethanolic organic compound was evaporated under vacuum to furnish the crude product. The product was washed with hot water three times, and there is no need for extra purification. All of the synthesized compounds were characterized by IR, NMR, and elemental analysis. The synthesized compounds are new and have been characterized completely.

9-(2-hydroxyphenyl)-3,3,6,6-tetramethyl-10-(4-(phenyldiazenyl) phenyl)-3,4,6,7,9, 10-hexahydroacridine-1,8 (2H, 5H)-dione (4f)

FT-IR (KBr, cm<sup>-1</sup>): 2956, 1646, 1607, 1507, 1463, 1379, 1142 cm<sup>-1</sup>. <sup>1</sup>H NMR (300 MHz, CDCl<sub>3</sub>): δ; 1.07 (6H, s), 1.17 (6H, s), 2.00 – 2.67 (8H, m), 4.72 (1H, s), 6.79 (2H, d, J = 8.5 Hz), 7.01 – 7.08 (3H, m), 7.15 – 7.18 (1H, m), 7.45 – 7.48 (1H, m), 7.50 – 7.57 (3H, m), 7.82 – 7.88 (2H, m), 7.95 – 7.98 (1H, m) ppm. <sup>13</sup>C NMR (75 MHz, CDCl<sub>3</sub>): δ; 200.90, 153.43, 151.98, 149.50, 145.57, 129.84, 129.11, 128.99, 128.15, 127.53, 125.12, 124.65, 124.38, 124.22, 122.88, 122.39, 118.37, 50.09, 41.67, 32.31, 31.89, 29.24, 28.43 ppm.

Anal.calcd. for C<sub>35</sub>H<sub>35</sub>N<sub>3</sub>O<sub>3</sub>: C, 77.10; H, 6.48; N, 7.78. Found: C, 77.04; H, 6.47; N, 7.70.

3,3,6,6-tetramethyl-9-(2-(butoxy) phenyl)-10-(4-

(phenyldiazenyl)phenyl)-3,4,6,7,9, 10-hexahydroacridine-1,8 (2H, 5H)-dione (6a)

FT-IR (KBr, cm<sup>-1</sup>): 3050 (Aromatic C–H stretching), 2978 (Aliphatic C–H stretching), 1662 (C=O stretching), 1605 (Aromatic C=C stretching), 1507 (N=N stretching), 1485 (Aromatic C=C stretching), 1368 (C–N stretching), 1210 (C–O stretching) cm<sup>-1</sup>. <sup>1</sup>H NMR (DMSO-d<sub>6</sub>, 600 MHz) δ 0.98–1.01 (brs, 9H), 1.04 – 1.07 (brs, 5H, Ha or Hf), 2.12 (s, 2H, Hb or Hc), 2.17–2.26 (brs, 2H), 2.30–2.39 (brs, 2H), 2.41–2.42 (brs, 2H), 4.53 (brs, 2H), 5.25 (s, 1H), 7.40–7.43 (m, 3H), 7.53–7.58 (m, 2H), 7.59–7.61 (m, 3H), 7.86 (d, J = 0.6 J = 14.4 Hz, 2H), 7.93–8.00 (m, 3H) ppm. <sup>13</sup>C NMR (DMSO-d<sub>6</sub>, 150 Hz): δc: 29.40, 32.18, 32.58, 46.40, 50.60, 55.63, 122.46, 122.64, 123.06, 123.80, 124.29, 125.26, 126.31, 129.98, 130.20, 131.68, 132.22, 139.90, 140.21, 149.00, 150.33, 196.62 (C=O) ppm. Anal. calcd. for C<sub>74</sub>H<sub>76</sub>N<sub>6</sub>O<sub>6</sub>: C, 77.52 H, 6.67; N, 7.34. Found: C, 77.59; H, 6.69; N, 7.34.

(8a) FT-IR (KBr, cm<sup>-1</sup>): 3045 (Aromatic C–H stretching), 2957 (Aliphatic C–H stretching), 1636 (C=O stretching), 1580 (Aromatic C=C stretching), 1528 (N=N stretching), 1409 (Aromatic C=C stretching), 1368 (C–N stretching), 1257 (C–O stretching) cm<sup>-1</sup>. <sup>1</sup>H NMR (DMSO-d<sub>6</sub>, 600 MHz): δ 0.97–0.98 (brs, 6H), 1.02–1.05 (brs, 8H), 1.87 (s, 3H), 2.04–2.12 (brs, 3H), 2.52–2.52 (brs, 2H), 3.60 (brs, 5H), 5.63 (s, 1H), 7.43 (d, J = 18.0 Hz, 3H), 7.48–7.53 (m, 1H), 7.55–7.59 (m, 3H), 7.86–7.90 (m, 3H), 7.93 (s, 2H) ppm. <sup>13</sup>C NMR (DMSO-d<sub>6</sub>, 150 MHz): δ 31.51, 32.50, 32.72, 42.56, 48.03, 50.65, 55.65, (two peaks), 113.87, 115.24, 122.17, 122.35, 122.82, 124.37, 125.61, 129.62, 129.88, 130.06, 131.56, 143.32 (two peaks), 147.98, 152.50, 159.27, 196.72 (C=O) ppm. Anal. calcd. for C<sub>76</sub>H<sub>80</sub>N<sub>6</sub>O<sub>8</sub>: C, 75.79 H, 6.71; N, 6.98. Found: C, 75.72; H, 6.69; N, 6.97.

(10) FT-IR (K BR, cm<sup>-1</sup>): 2956 (Aliphatic C–H stretching), 1716, 1662, 1600, 1576, 1503, 1459, 1266, 1223, 1194 cm<sup>-1</sup>. <sup>1</sup>H NMR (DMSO-d<sub>6</sub>, 300 MHz): δ 0.92–1.01 (brs, 18H), 1.24–1.29 (brs, 18H), 1.93–2.14 (brs, 8H), 2.24–2.29 (brs, 8H), 2.46–2.58 (brs, 8H), 3.74 (s, 6H), 3.76 (s, 3H), 5.27 (s, 3H), 6.56 (d, J = 1.9 Hz-z J = 8.5 Hz, 2H), 6.65 (d, J = 7.8 Hz, 2H), 6.72 (d, J = 3.4 Hz, 2H), 6.82 (brs, 3H), 7.00 – 7.06 (m, 3H), 7.14 (d, J = 8.3 Hz, 3H), 7.22–7.26 (m, 2H), 7.37–7.45 (m, 3H), 7.52–7.60 (m, 8H), 7.67, (d, J = 8.2 Hz, 3H), 7.85–7.89 (m, 3H), 7.93 (d, J = 7.8 Hz, 2H) ppm. <sup>13</sup>C NMR (DMSO-d<sub>6</sub>, 75 MHz): δ 28.43, 29.24, 32.26 (two peaks), 50.15, 64.50, 114.69, 115.22, 115.47, 120.75, 122.39, 122.77, 122.85, 123.66, 124.41, 129.69, 129.78, 129.84, 135.90, 145.43, 147.36, 152.51, 163.00, 196.25 ppm. Anal. calcd. for C<sub>111</sub>H<sub>108</sub>N<sub>12</sub>O<sub>12</sub>: C, 73.95; H, 6.01; N, 9.30. Found: 73.98; H, 6.04; N, 9.33.

Full experimental detail, <sup>1</sup>H and <sup>13</sup>C NMR spectra of all products can be found via the “Supplementary Information” section of this article’s webpage.

## 3. Results and discussion

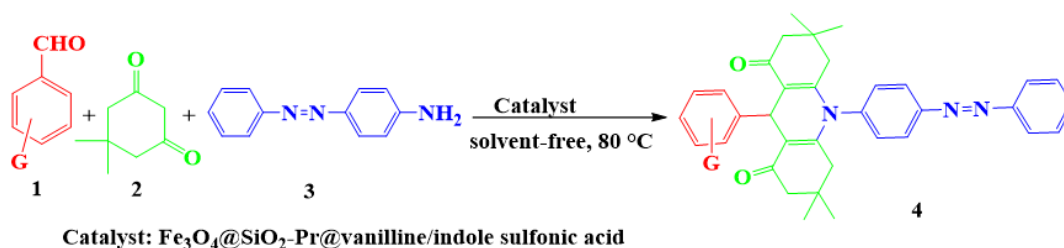
### 3.1 Synthesis and identification of the catalyst

In continuation of our efforts in designing greener heterogeneous catalysts [35, 36] and synthesis of new organic

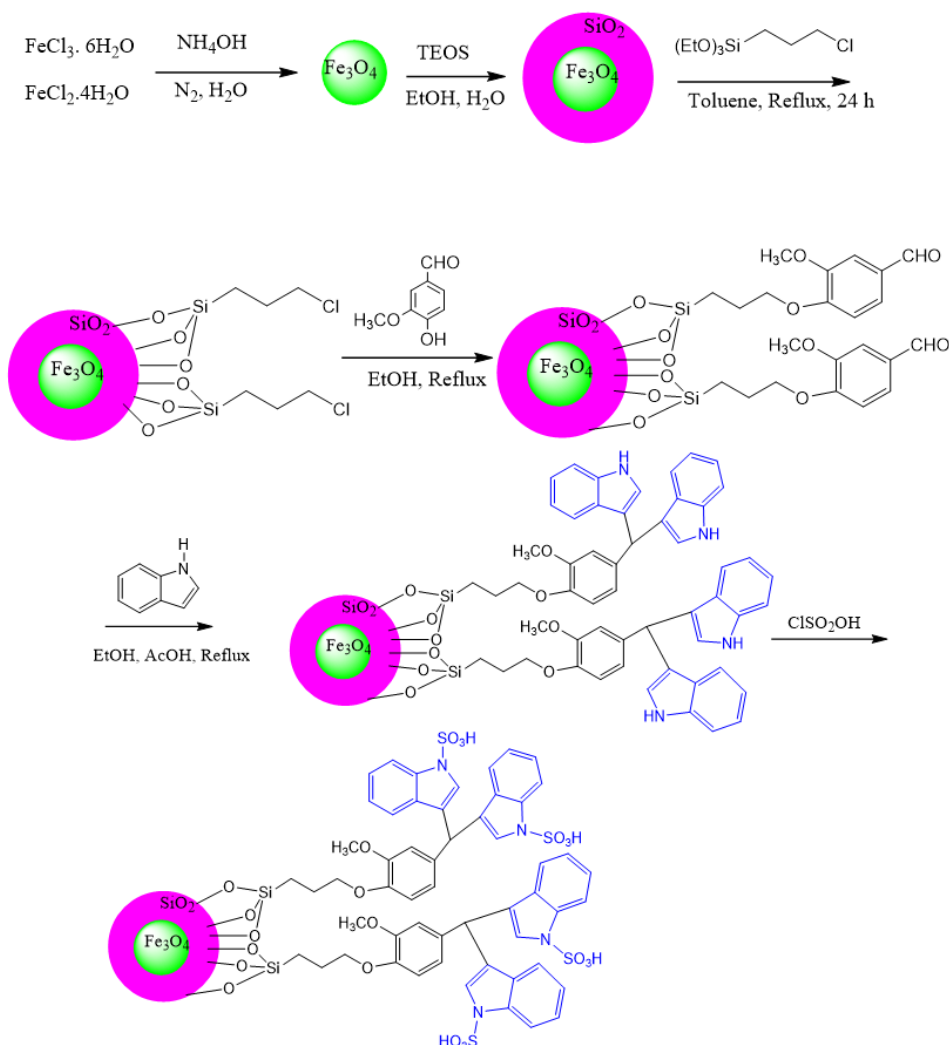
compounds [37, 38], we herein present the preparation of  $\text{Fe}_3\text{O}_4@ \text{SiO}_2\text{Pr}@ \text{Vanillin}@ \text{Indole}$ -sulfonic acid and its application as new, green and efficient nanomagnetic catalyst for the multicomponent reaction for the synthesis of azo-derived DHPs (Scheme 1).

Initially, nanoparticles were synthesized via multi-step reactions as shown in Scheme 2.  $\text{Fe}_3\text{O}_4$  MNPs were synthesized by co-precipitation of ferrous ( $\text{Fe}^{2+}$ ) and ferric ( $\text{Fe}^{3+}$ ) ions [39, 40]. Then,  $\text{Fe}_3\text{O}_4@ \text{SiO}_2$  NPs were synthesized via the reaction of  $\text{Fe}_3\text{O}_4$  with the tetraethyl orthosilicate (TEOS) in the presence of ammonia solution. In the next step, the reaction of  $\text{Fe}_3\text{O}_4@ \text{SiO}_2$  nanoparticles with (3-chloropropyl) triethoxysilane (CPTES) in dry

toluene under a nitrogen atmosphere led to  $\text{Fe}_3\text{O}_4@ \text{SiO}_2\text{-(CH}_2\text{)}_3\text{Cl}$  MNPs. The resulting  $\text{Fe}_3\text{O}_4@ \text{SiO}_2\text{-(CH}_2\text{)}_3\text{Cl}$  NPs were reacted with vanillin followed by the reaction with 2 equivalent of indole under refluxing EtOH in the presence of 10 drops of acetic acid to prepare  $\text{Fe}_3\text{O}_4@ \text{SiO}_2\text{-Pr}@ \text{vanilline}/\text{indole}$ .  $\text{Fe}_3\text{O}_4@ \text{SiO}_2\text{-Pr}@ \text{vanilline}/\text{indole}$  NPs were treated with chlorosulfonic acid to synthesize  $\text{Fe}_3\text{O}_4@ \text{SiO}_2\text{-Pr}@ \text{vanilline}/\text{indole}$ -sulfonic acid. The structure of  $\text{Fe}_3\text{O}_4@ \text{SiO}_2\text{-Pr}@ \text{vanilline}/\text{indole}$  sulfonic acid MNPs was established entirely by different analysis such as FT-IR, XRD, SEM, TEM, TGA, VSM and EDAX. The FT-IR spectra of  $\text{Fe}_3\text{O}_4@ \text{SiO}_2\text{-Pr}@ \text{vanilline}/\text{indole}$  sulfonic acid MNPs are shown in figure 2. The signals of



**Scheme 1.** Multicomponent synthesis of azo-derived DHPs.



**Scheme 2.** Multi-step synthesis of  $\text{Fe}_3\text{O}_4@ \text{SiO}_2\text{-Pr}@ \text{Vanilline}/\text{indole}$  sulfonic acid.

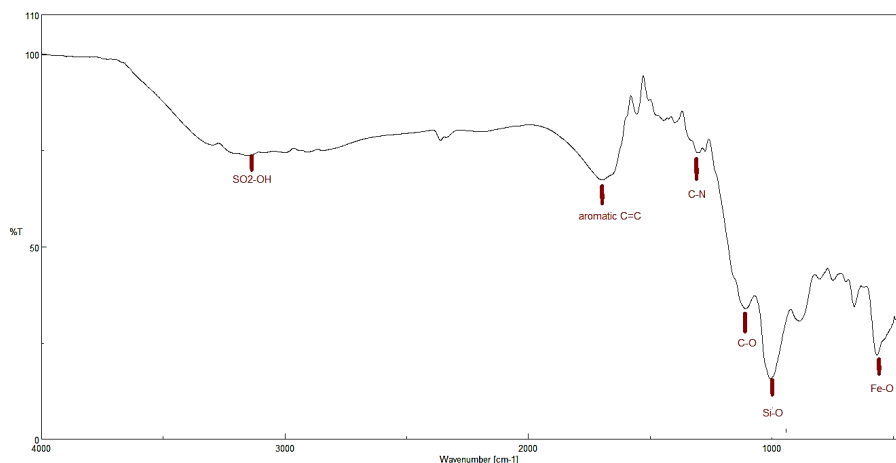


**Figure 2.** FT-IR spectrum of synthesized  $\text{Fe}_3\text{O}_4@SiO_2\text{-Pr@vanilline/indole}$  sulfonic acid MNPs.

stretching vibrations of aromatic  $\text{C}=\text{C}$ ,  $\text{C}-\text{N}$  and  $\text{C}-\text{O}$  were appeared in  $1589\text{ cm}^{-1}$ ,  $1302\text{ cm}^{-1}$  and  $1227\text{ cm}^{-1}$ , respectively. The  $\text{SO}_2\text{-OH}$  stretching vibration was shown as a broad signal in  $2750 - 3367\text{ cm}^{-1}$ . The presence of  $\text{Fe}_3\text{O}_4@SiO_2\text{-Pr}$  in this synthesized catalyst can be confirmed by the  $\text{Fe}-\text{O}$  stretching vibration at  $552\text{ cm}^{-1}$  and  $\text{Si}-\text{O}$  at  $1005\text{ cm}^{-1}$ , respectively that shows the successful functionalization of the  $\text{Fe}_3\text{O}_4$  with tetraethyl orthosilicate.  $\text{C}-\text{N}$  stretching signal at  $1302\text{ cm}^{-1}$  is indicative of immobilization of indole on the surface of  $\text{Fe}_3\text{O}_4@SiO_2@CPTES$  NPs.

X-ray powder diffraction patterns (XRD) of  $\text{Fe}_3\text{O}_4@SiO_2\text{-Pr@vanilline/indole}$  sulfonic acid MNPs were shown in figure 3. The diffraction peaks at  $2\theta = 35.6^\circ$ ,  $43.1^\circ$ ,  $51.6^\circ$ ,  $57.3^\circ$ ,  $63.7^\circ$  and  $67.2^\circ$  were related to planes of  $\text{Fe}_3\text{O}_4$ , respectively. These data indicate that the  $\text{Fe}_3\text{O}_4$  nanoparticles have a cubic face-centered (fcc) lattice. This XRD values are in accordance to XRD of standard  $\text{Fe}_3\text{O}_4$  (JCPDS CARD NO. 19-629). On the other hand, the broadening of XRD spectra at  $2\theta = 13 - 30^\circ$  is related to the surrounding of the nano magnetic by the silica layer.

The crystalline size of the prepared nanomaterials was cal-

culated using Debye-Scherrer's formula given in Eq. (1),

$$D = \frac{K\lambda}{\beta \cos \theta} \quad (1)$$

where,  $D$ ,  $K$ ,  $\lambda$ ,  $\beta$ , and  $\theta$  are the crystalline size, constant, wavelength, full-width half maximum (FWHM), and diffraction angle, respectively. The crystalline size was calculated to be  $0.25\text{ \AA}$ .

FE-SEM and TEM images of  $\text{Fe}_3\text{O}_4@SiO_2\text{-Pr@vanilline/indole}$  sulfonic acid nanoparticles (figure 4) showed the particle size distributions and morphologies of these Nps.  $\text{Fe}_3\text{O}_4@SiO_2\text{-Pr@vanilline/indole}$  sulfonic acid nanoparticles are spherical with size distributions of 18.82, 20.10, and 38.95 nm with suitable aggregation. The structure and the size of the  $\text{Fe}_3\text{O}_4@SiO_2\text{-Pr@vanilline/indole}$  sulfonic acid nanoparticles were obvious in figure 4. Also, the structure of the nanoparticles was confirmed by observing dark spots within the gray spherical silica layer. EDX analysis established the synthesis of  $\text{Fe}_3\text{O}_4@SiO_2\text{-Pr@vanilline/indole}$  sulfonic acid nanoparticles based on the presence of Fe (18%), O (45%), Si (23%), C (56%), and S (29%) in the spectra as shown in figure 5. The presence of sulfur in the EDX analysis is indicative that the catalyst was sulfonated by chlorosulfonic acid.

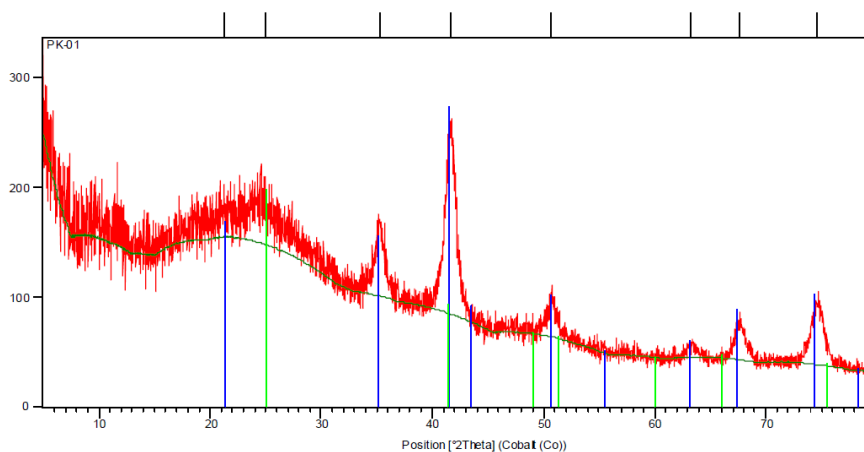


**Figure 3.** XRD diffraction spectra of  $\text{Fe}_3\text{O}_4@SiO_2\text{-Pr@vanilline/indole}$  sulfonic acid MNPs.

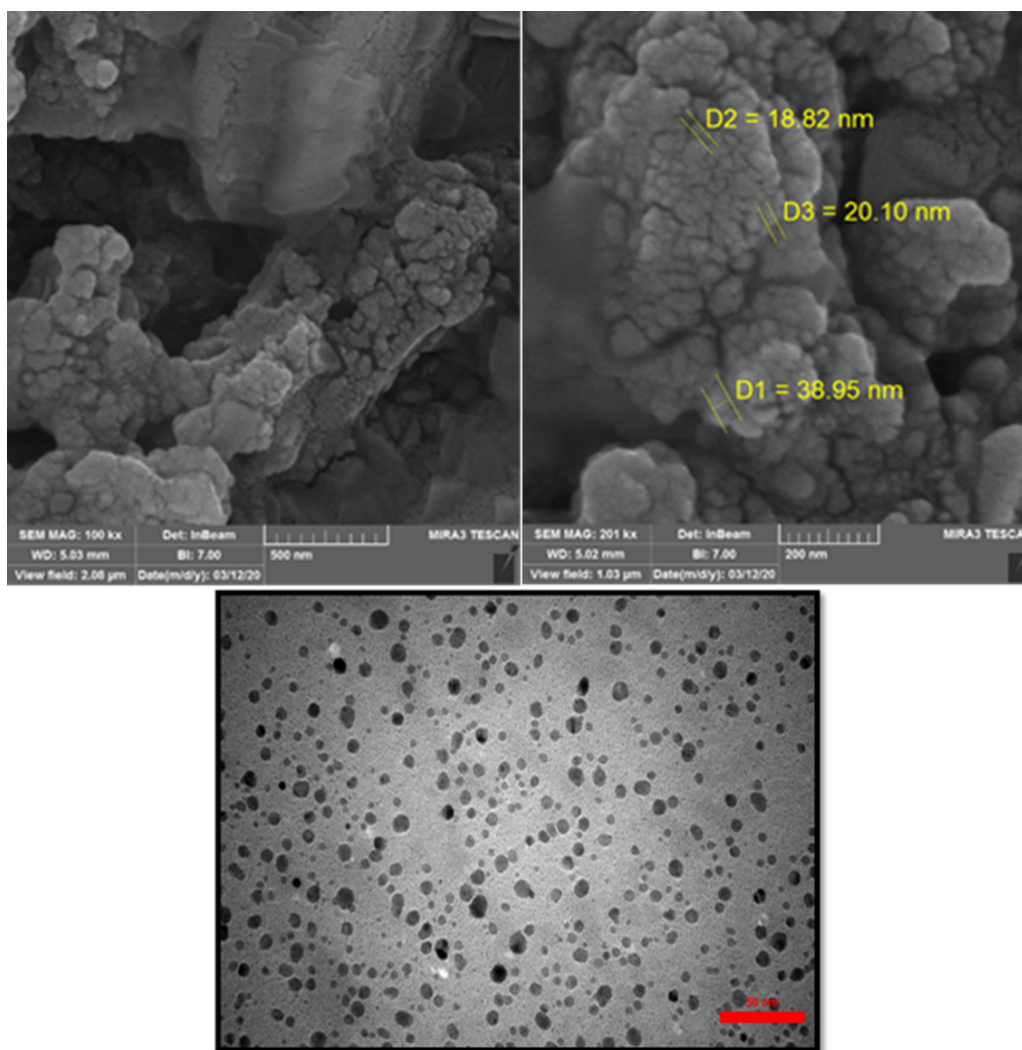


**Figure 4.** (up) FE-SEM image of  $\text{Fe}_3\text{O}_4@SiO_2\text{-Pr@vanilline/indole sulfonic acid}$  nanoparticles (down) TEM image.

Figure 6 shows the TGA curves of  $\text{Fe}_3\text{O}_4@SiO_2\text{-Pr@vanilline/indole sulfonic acid}$ . Two weight-loss steps are observed for  $\text{Fe}_3\text{O}_4@SiO_2\text{-Pr@vanilline/indole sulfonic acid}$ . First weight-loss related to desorption of

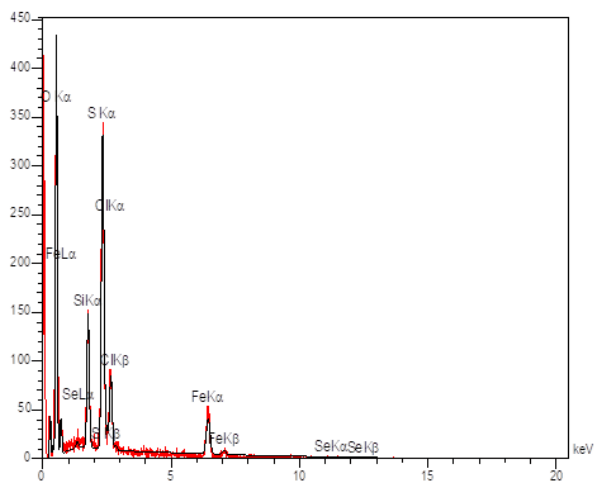


**Figure 5.** EDX analysis of  $\text{Fe}_3\text{O}_4@SiO_2\text{-Pr@vanilline/indole sulfonic acid}$ .

water from the catalyst which is observed between  $117^\circ\text{C}$  and the second weight-loss step between  $184^\circ\text{C}$  and  $368^\circ\text{C}$  is due to the decomposition of organic compounds.

Vibrating sample magnetometry (VSM) is a method by which hysteresis loops ( $m$  vs.  $H$ ) may be accurately measured. The process is to apply a field across a sample and to measure the moment induced in the sample along the field direction by oscillating the sample near a set of pick-up coils. The VSM curve of nano magnetic,  $\text{Fe}_3\text{O}_4@SiO_2\text{-pr}$  and  $\text{Fe}_3\text{O}_4@SiO_2\text{-Pr@vanilline/indole sulfonic acid}$  was evaluated as shown in figure 7. The value confirmed that the superparamagnetic properties of the synthesized MNPs is sufficient for a magnetic separation with a conventional magnet. On the other hand, the data showed that the long addition of the catalyst chair led to a decrease in the value of magnetization.

To evaluate of acidity of synthesized catalyst, titration of 10 mL of aqueous solution of catalyst (0.100 M) with 0.100 M of NaOH was carried out. The titration curve is given in figure 8. As shown in figure 8, the catalyst was neutralized with 6 mL of 0.100 M of NaOH. According to the data of the titration curve, the value of  $pK_a$  is 5.85.

To investigate the efficiency of  $\text{Fe}_3\text{O}_4@SiO_2\text{-}$

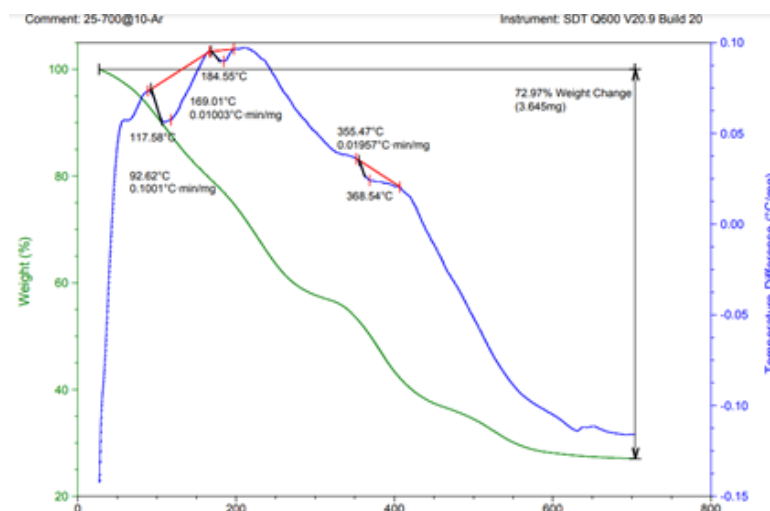


Figure 6. TGA-DTA analysis of  $\text{Fe}_3\text{O}_4@SiO_2\text{-Pr@vanilline/indole sulfonic acid}$ .

Pr@vanilline/indole sulfonic acid as a green and effective catalyst for the promotion of organic transformation, the reaction of 4-nitrobenzaldehyde, dimedone, and 4-aminoazobenzene was selected as a model reaction (Table 1). The sample reaction, at first, was carried out in the absence of any catalyst. The reaction leads to a trace amount of product after 24 h. It established the reaction needs catalyst for promotion forward. Then, the sample reaction was carried out in the presence of the catalytic amount of concentrated HCl, KSF,  $\text{Fe}_3\text{O}_4$ ,  $\text{SiO}_2$ , l-proline, [Bmim]Br, nano- $\text{Fe}_3\text{O}_4$ ,  $\text{Fe}_3\text{O}_4@SiO_2\text{-Pr}$ , and  $\text{Fe}_3\text{O}_4@SiO_2\text{-Pr@vanilline/indole sulfonic acid}$ . The results showed that the superior catalyst for this reaction is  $\text{Fe}_3\text{O}_4@SiO_2\text{-Pr@vanilline/indole sulfonic acid}$  due to its Lewis and Bronsted character. To find the suitable solvent for this reaction, the sample reaction was carried out in  $\text{CHCl}_3$ ,  $\text{CH}_2\text{Cl}_2$ , EtOH,  $\text{H}_2\text{O}$  under reflux condition and under solvent-free condition. The reaction under solvent-free conditions gained more product in a shorter reaction time. To control the catalyst loading effect on the

sample reaction, the amounts of 0.01 g, 0.03 g, 0.05 g, and 0.1 g of catalyst were checked. The results indicate that the optimum amount of catalyst per 1 mmol of aldehyde is 0.05 g. The higher amount didn't lead to higher productivity in shorter reaction time. The results are shown in Table 1. It was checked the reaction in the absence of any catalyst led to trace amounts of product after 24 hours. It shows the presence of catalyst is essential for this reaction.

With the best conditions in hands, we synthesis various azo-linked acridines through the three-component reaction of arylaldehydes, dimedone and 4-aminoazobenzene in the presence of 0.05 g of  $\text{Fe}_3\text{O}_4@SiO_2\text{-Pr@vanilline/indole sulfonic acid}$  Nps under solvent-free condition. The results were shown in Table 2. As shown in Table 2, the aryl aldehyde with electron-donating substituents reacted in a higher reaction time with lower yields due to the nucleophilic addition character of the reaction.

In continuation of our effort, we triggered to synthesize bis-azo-linked acridines via the reaction of synthesized bis aldehydes, dimedone and 4-aminoazobenzene in the optimized reaction condition. The results were shown in Table 3. The Scheme 3 shows the structure of starting materials and product.

To expand the generality of method, we triggered to synthesize star-like tris azo-linked acridines for the first time. In this endeavor, we used extra amount of dimedone and azobenzene to synthesize tris molecules. The structure of tris azo-acridine was shown in Scheme 4.

Hot filtration was utilized to determine the efficiency of

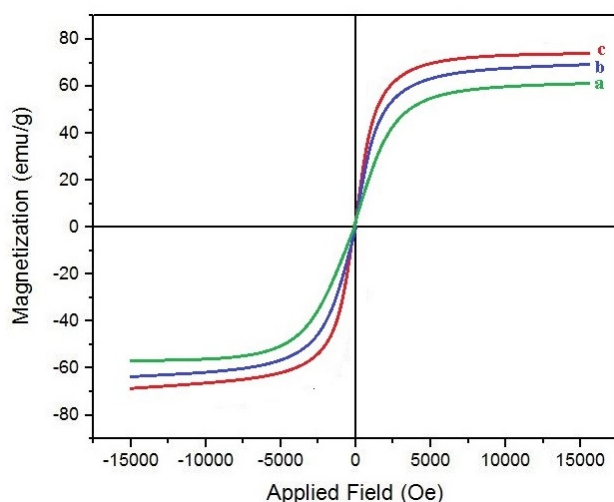


Figure 7. Magnetization curve of (a)  $\text{Fe}_3\text{O}_4@SiO_2\text{-Pr@vanilline/indole sulfonic acid}$ , (b)  $\text{Fe}_3\text{O}_4@SiO_2\text{-Pr}$  and (c)  $\text{Fe}_3\text{O}_4$ .

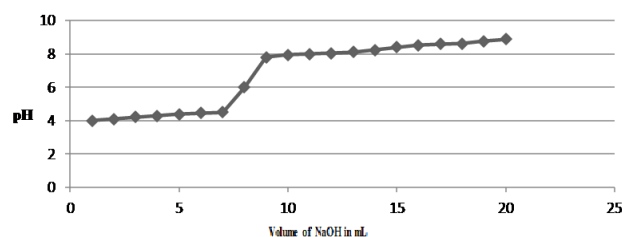


Figure 8. The titration curve for the titration of the catalyst.

**Table 1.** Optimization of multi-component synthesis of acridine 4a.

Catalyst	Catalyst amount/1mmol of substrate	Reaction condition	Time (h or min)	Yield (%)
-	-	Reflux in EtOH	24 h	trace
HCl	10 drops	Reflux in EtOH	12 h	23
KSF	0.1 g	Reflux in EtOH	8 h	37
Fe <sub>3</sub> O <sub>4</sub>	0.1 g	Reflux in EtOH	6 h	43
l-proline	0.1 g	Reflux in EtOH	8 h	34
SiO <sub>2</sub>	0.1 g	Reflux in EtOH	6 h	42
[Bmim]Br	3 mL	Heating at 80 °C	7 h	39
Nano-Fe <sub>3</sub> O <sub>4</sub>	0.05	Reflux in EtOH	4 h	74
Fe <sub>3</sub> O <sub>4</sub> @SiO <sub>2</sub> -Pr Nps	0.05 g	Reflux in EtOH	4 h	84
Fe <sub>3</sub> O <sub>4</sub> @SiO <sub>2</sub> -Pr@vanilline/indole sulfonic acid	0.05 g	Reflux in EtOH	40 min	95
Fe <sub>3</sub> O <sub>4</sub> @SiO <sub>2</sub> -Pr@vanilline/indole sulfonic acid	0.05 g	Reflux in CH <sub>2</sub> Cl <sub>2</sub>	2 h	87
Fe <sub>3</sub> O <sub>4</sub> @SiO <sub>2</sub> -Pr@vanilline/indole sulfonic acid	0.05 g	Reflux in CHCl <sub>3</sub>	2	91
Fe <sub>3</sub> O <sub>4</sub> @SiO <sub>2</sub> -Pr@vanilline/indole sulfonic acid	0.05 g	Reflux in water	40 min	93
Fe <sub>3</sub> O <sub>4</sub> @SiO <sub>2</sub> -Pr@vanilline/indole sulfonic acid	0.05 g	Solvent-free, 80 °C	15 min	98
Fe <sub>3</sub> O <sub>4</sub> @SiO <sub>2</sub> -Pr@vanilline/indole sulfonic acid	0.01 g	Solvent-free, 80 °C	60 min	88
Fe <sub>3</sub> O <sub>4</sub> @SiO <sub>2</sub> -Pr@vanilline/indole sulfonic acid	0.03 g	Solvent-free, 80 °C	45 min	91
Fe <sub>3</sub> O <sub>4</sub> @SiO <sub>2</sub> -Pr@vanilline/indole sulfonic acid	0.1 g	Solvent-free, 80 °C	12 min	98

the nanocatalyst. 4-Nitrobenzaldehyde, dimedone, and 4-aminoazobenzene were reacted using a nanocatalyst for 5 min, and then the nanocatalyst was removed from the reaction mixture. After heating of the filtrate and checking the reaction by TLC, we observed that only a partial progress happened in the reaction and it means the nanocatalyst is essential for the reaction progress.

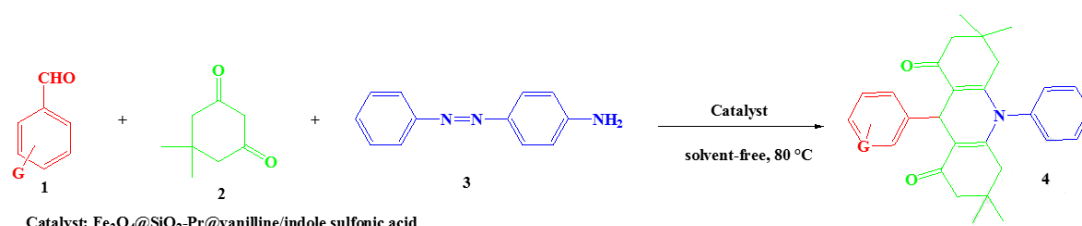
The reusability of the catalyst was checked as shown in figure 9. After completion of the sample reaction as indicated by TLC (1: 4 EA: n-hexane), the reaction mixture was dissolved in 10 mL hot EtOH. The catalyst was insoluble in EtOH, and after filtration, the catalyst was separated from the reaction mixture. It was dried in an oven at 120 °C for 4 hours and was recycled and reused for the next reaction. The FE-SEM image of the recycled nano catalyst and data in figure 8 established that the catalyst can be recycled for 6 runs without any sustainable decrease in reaction yield. The amount of catalyst reused in each run was shown in Table 4.

After study of recycling of Fe<sub>3</sub>O<sub>4</sub>@SiO<sub>2</sub>-Pr@vanilline/indole sulfonic acid Nps, finally turn

over number (TON) and turn over frequency (TOF) of the present catalyst were also calculated for the model reaction based on the synthesis of 4a; they were found to be 546.32 and 351.66 h<sup>-1</sup>, respectively.

As a proposed mechanistic pathway, Fe<sub>3</sub>O<sub>4</sub>@SiO<sub>2</sub>-Pr@vanilline/indole sulfonic acid Nps can act as Lewis acid in inner layers and as an effective Bronsted acid via SO<sub>3</sub>H functional group surrounded the nanoparticles surface. Fe<sub>3</sub>O<sub>4</sub>@SiO<sub>2</sub>-Pr@vanilline/indole sulfonic acid Nps catalyzes the formation of oxonium ion with the aldehyde and helps to form carbanion from dimedone to facilitate Knoevenagel condensation between aldehyde and dimedone to synthesize chalcone. Then, the second equivalent of dimedone can attack to chalcone via Michael addition. Enolization and the addition of azoaniline can lead to the product (Scheme 5). To compare the efficiency of this method with previous reported methods, some studies were carried out (Table 5).

Highlighted points of this work is 1) synthesized azo-linked acridines are new. 2) The catalyst synthesized is completely new. 3) There is the first report for the synthesis

**Table 2.** The scope of multicomponent reaction in the presence of Fe<sub>3</sub>O<sub>4</sub>@SiO<sub>2</sub>-Pr@vanilline/indole sulfonic acid Nps.


Catalyst: Fe<sub>3</sub>O<sub>4</sub>@SiO<sub>2</sub>-Pr@vanilline/indole sulfonic acid

Entry	G	Product	Time (min)	Yield (%) <sup>a, b</sup>	Mp (°C) found
1	4-N,N-dimethylamino	4a	40	89	270-272
2	4-hydroxy,3,5-dimethoxy	4b	35	91	305-307
3	4-Cyano	4c	15	97	301-303
4	4-fluoro	4d	20	96	311-312
5	2,4-dihydroxy	4e	35	91	285-287
6	2-hydroxy	4f	30	93	300-302
7	3-Fluoro	4g	17	95	305-306
8	4-Bromo	4h	20	97	268-270
9	4-Chloro	4i	20	96	271-273
10	4-Nitro	4j	15	98	> 300
11	Styryl	4k	20	92	256-257
12	1-naphthalenecarbaldehyde	4l	25	90	231-233
13	thiophen	4m	20	91	189-191

<sup>a</sup>. Isolated yield. <sup>b</sup>. All of the compounds were characterized by mp, IR, NMR, and elemental analysis.

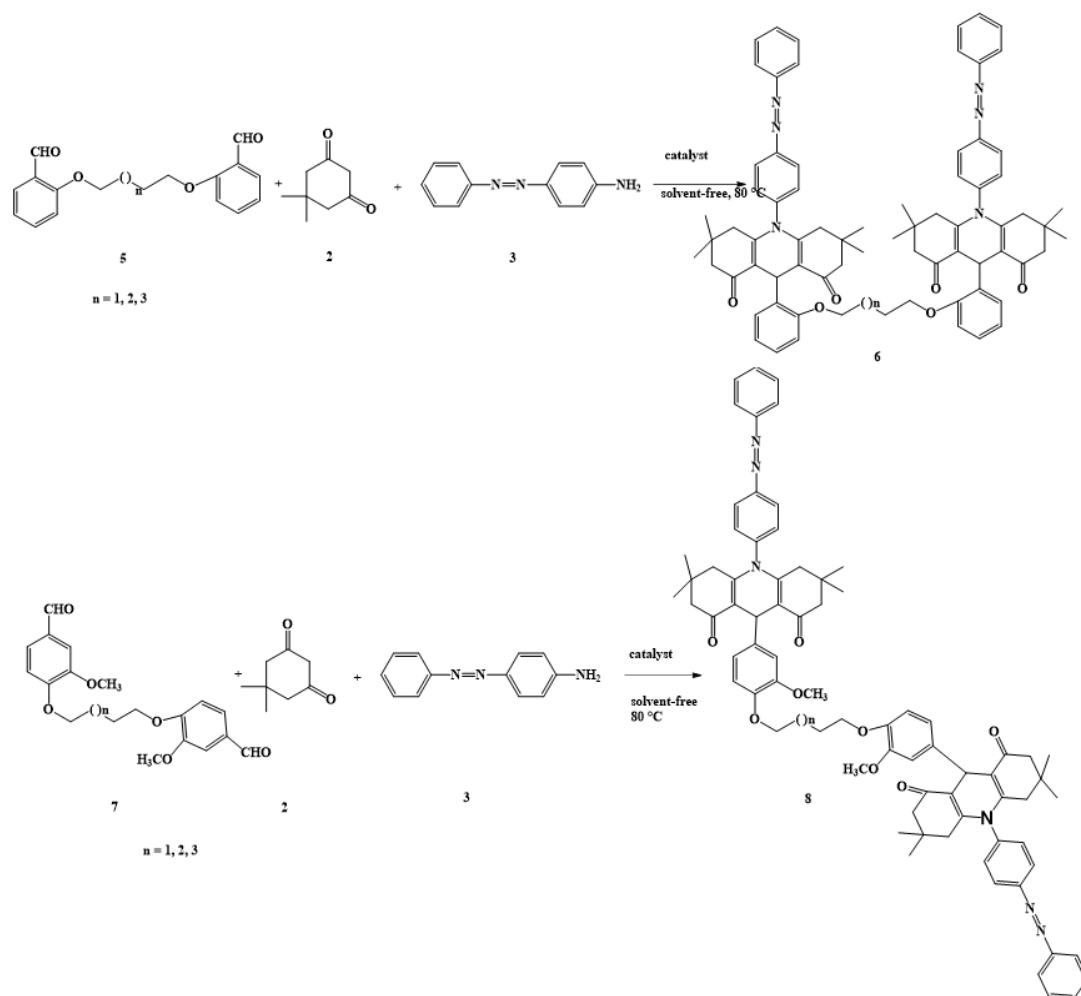
of azo-linked dihydropyridines using Fe<sub>3</sub>O<sub>4</sub>@SiO<sub>2</sub>-Pr@vanilline/indole sulfonic acid. 4) Shorter reaction time and higher yield, rather than most of the reported methods, are two major benefits of this work. 5) The reaction was carried out under solvent-free conditions, and

there is no need to use organic and hazardous solvents in this procedure. 6) The reaction was carried out at room temperature that need no heating and it is based on green chemistry rules because is energy-economical.

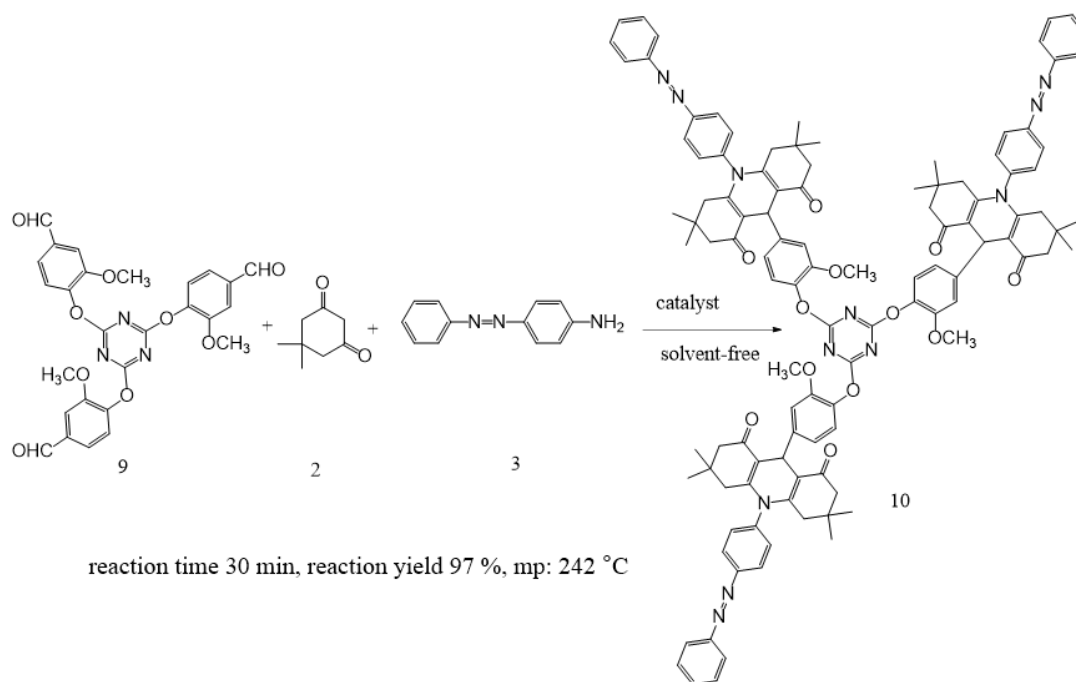
**Table 3.** Synthesis of bis azo-linked acridines using Fe<sub>3</sub>O<sub>4</sub>@SiO<sub>2</sub>-Pr@vanilline/indole sulfonic acid Nps.

Entry	n	Product	Time (min)	Yield (%) <sup>a, b</sup>	Mp (°C)
1	4	6a	20	97	196-198
2	5	6b	15	98	217-218
3	6	6c	20	94	195-197
4	4	8a	20	95	267-268
5	5	8b	15	97	276-278
6	6	8c	20	95	214-215

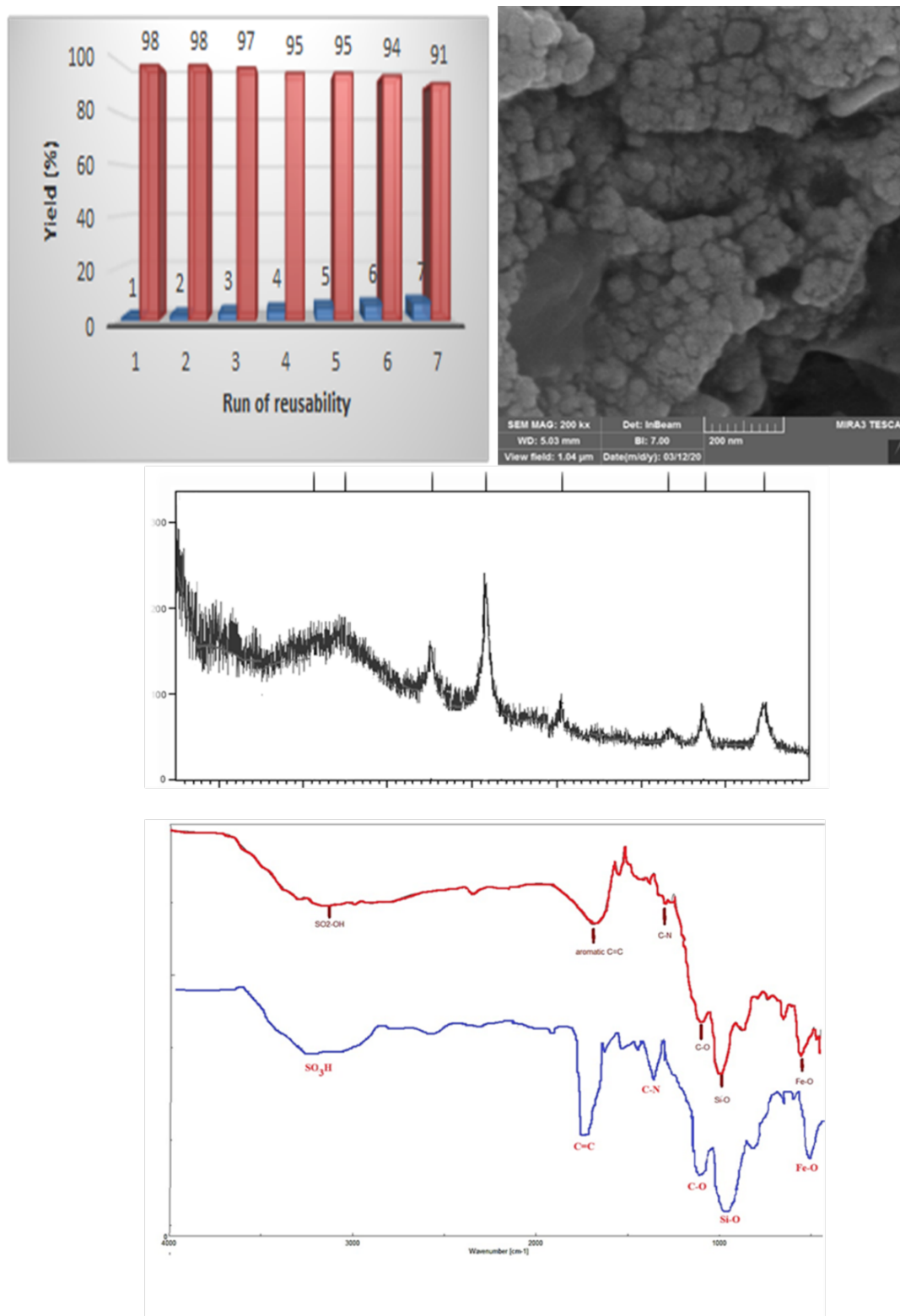
<sup>a</sup>. Isolated yield. <sup>b</sup>. All of the synthesized compounds are new and were characterized by IR, NMR, and elemental analysis.



**Scheme 3.** Synthesis of bis-azo-linked acridines using  $\text{Fe}_3\text{O}_4@\text{SiO}_2\text{-Pr@vanilline/indole sulfonic acid Nps}$ .



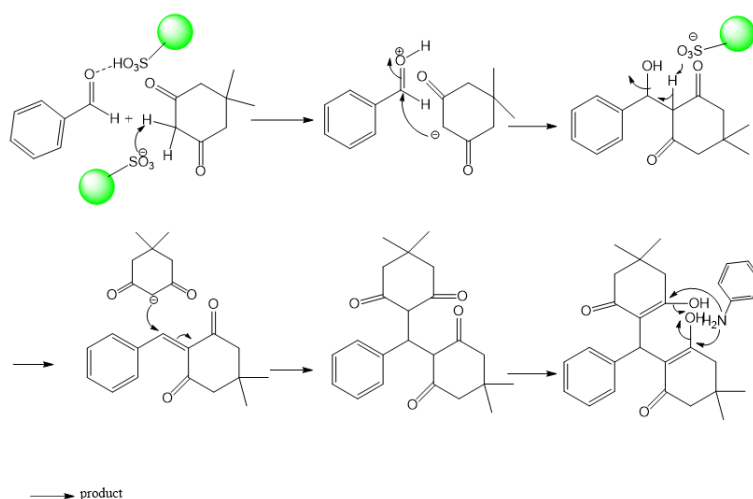
**Scheme 4.** Synthesis of tris-azo-linked DHPs  $\text{Fe}_3\text{O}_4@\text{SiO}_2\text{-Pr@vanilline/indole sulfonic acid Nps}$ .



**Figure 9.** Left: Reusability chart of  $\text{Fe}_3\text{O}_4@ \text{SiO}_2\text{-Pr@vanilline/indole sulfonic acid Nps}$ . Right: FE-SEM image of reused catalyst in 6th run, XRD and FT-IR of fresh (red curve) and reused catalyst after 6 runs (blue curve).

**Table 4.** The amount of catalyst reused in each run.

Run1	Run2	Run3	Run4	Run5	Run6
0.05 g	0.05 g	0.0476	0.472	0.4569	0.4550

**Scheme 5.** Proposed mechanism for the synthesis of DHPs.**Table 5.** Comparison of this method with reported methods.

Product	Catalyst (catalyst loading)	Condition	Time	Yield (%)	Run of reusability	Ref.
	Hollow Fe <sub>3</sub> O <sub>4</sub> @Dopamine SO <sub>3</sub> H (0.01 g)	Solvent-free, 100 °C	40 min	85%	6	[39]
	chitosan magnetic nanocomposite Ch-Rhomboclase NCs (1.8 mol%)	Solvent-free, 80 °C	120 min	86%	7	[40]
	Fe <sub>3</sub> O <sub>4</sub> NPs (0.024 g)	Solvent-free, 80 °C	5 min	92%	5	[41]
	Fe <sub>3</sub> O <sub>4</sub> -Pectin-1-amino- 8-naphthol-3,6-disulfonic acid (0.035)	EtOH, ultrasonic bath (frequency: 60 Hz, power density: 100 W, 40 °C)	15 min	95%	5	[42]
	Glutathione-Coated Magnetic NPs (0.2g)	Solvent-free, 110 °C	30 min	91%	3	[43]
4d	Fe <sub>3</sub> O <sub>4</sub> @SiO <sub>2</sub> -Pr@vanilline/ indole sulfonic acid	Solvent-free, rt	25	98	6	This work

## 4. Conclusions

In this research, synthesis, characterization, and the application of the new nanocatalyst ( $\text{Fe}_3\text{O}_4@\text{SiO}_2\text{-pr@vanilline/Indole sulfonic acid}$ ) have been presented. It was fully characterized using FT-IR, XRD, SEM, TEM, EDS, TGA-DTG, and VSM analysis. An environmentally friendly method has been developed for the preparation of azo-linked acridines, bis azoacridines, and tris azoacridines by  $\text{Fe}_3\text{O}_4@\text{SiO}_2\text{-pr@vanilline/Indole sulfonic acid}$  under solvent-free conditions. The promising points of this work are the mild conditions, short reaction time, and reusability of the catalyst, as well as the high yield and easy work-up. In this work, we carried out the reaction under solvent-free condition that needs no organic solvents as media. Organic solvents are poisonous and dangerous, the risk of using of organic solvent can decrease in this method. Usage of room temperature in this reaction condition helps saving the energy and it is based on green chemistry rules. For the future, it will be interesting to estimate the biological activity of this category of compounds in vitro and in vivo analysis. Maybe, they are the azo-dyes that can act as antibacterial or anticancer, etc. It was suggested that, in the future, this work can be accelerated under microwave conditions or under ultrasound irradiation to give better results.

### Authors contributions

Authors have contributed equally in preparing and writing the manuscript.

### Availability of data and materials

The data that support the findings of this study are available from the corresponding author, upon reasonable request.

### Conflict of interests

The author declare that they have no known competing financial interests or personal relationships that could have appeared to influence the work reported in this paper.

## References

- [1] M. Erşatır, M. Türk, E. S. Giray, and J. Supercrit. *Fluids*, **176**(2021): 105303–105310. DOI: <https://doi.org/10.1016/j.supflu.2021.105303>.
- [2] S. Ghosh, F. Saikh, J. Das, and A. K. Pramanik. *Tetrahedron Lett.*, **54**(2013):58–62. DOI: <https://doi.org/10.1016/j.tetlet.2012.10.079>.
- [3] L. Z. Fekri, M. Nikpassand, and K. H. Pour. *Curr. Org. Synth.*, **12**(2015):76–79. DOI: <https://doi.org/10.2174/1570179411666140806005614>.
- [4] M. Rucins, A. Plotniece, E. Bernotiene, W. B. Tsei, and A. Sobolev. *Catalysts*, **10**(2020):1019–1040. DOI: <https://doi.org/10.3390/catal10091019>.
- [5] M. Mokhtary and S. A. Mirfarjood Langroudi. *Monatshefte Chem.*, **145**(2014):1489–1494. DOI: <https://doi.org/10.1007/s00706-014-1206-9>.
- [6] G. Pan, Ch. He, M. Chen, Q. Xiong, W. Cao, and X. Feng. *CCS Chem.*, **4**(2022):2000–2008. DOI: <https://doi.org/10.31635/ccschem.021.202101060>.
- [7] R. M. Vala and H. M. Patel. *Adv. Heterocycl. Chem.*, **141**(2023): 179–208. DOI: <https://doi.org/10.1016/bs.aihch.2023.04.001>.
- [8] P. Kumar, A. Kumar, and Kh. Hussain. *Ultrason. Sonochem.*, **19**(2012):729–735. DOI: <https://doi.org/10.1016/j.ultsonch.2011.12.021>.
- [9] M. Nasr-sfahani, S. J. Hoseini, M. Montazerzohori, R. Mehrabi, and H. Nasrabadi. *J. Mol. Catal. A: Chem.*, **382**(2014):99–105. DOI: <https://doi.org/10.1016/j.molcata.2013.11.010>.
- [10] K. Purandhar, V. Jyothi, P. P. Reddy, M. A. Chari, and K. Mukkanti. *J. Heterocycl. Chem.*, **49**(2012):232–236. DOI: <https://doi.org/10.1002/jhet.793>.
- [11] S. Sheik Mansoor, K. Aswin, K. Logaiya, S. P. N. Sudhan, and J. King Saud. *Univ. Sci.*, **25**(2013):191–199. DOI: <https://doi.org/10.1016/j.jksus.2013.02.001>.
- [12] S. S. Mansoor, K. Aswin, K. Logaiya, and S. P. N. Sudhan. *Arab. J. Chem.*, **10**(2017):S546–S553. DOI: <https://doi.org/10.1016/j.arabjc.2012.10.017>.
- [13] S. Sheik Mansoor, K. Aswin, K. Logaiya, and S. P. N. Sudhan. *J. Saudi Chem. Soc.*, **20**(2016):S100–S108. DOI: <https://doi.org/10.1016/j.jscs.2012.09.010>.
- [14] G. B. Dharma Rao, S. Nagakalyan, G. K. Prasad, G. B. Dharma, and G. K. Prasad. *RSC Adv.*, **7**(2017):3611–3616. DOI: <https://doi.org/10.1039/C6RA26664A>.
- [15] R. Kumar, N. H. Andhare, A. Shard, Richa, and A. K. Sinha. *RSC Adv.*, **4**(2014):19111–19121. DOI: <https://doi.org/10.1039/C4RA02169J>.
- [16] R. C. Cioc, E. Ruijter, and R. V. A. Orru. *Green Chem.*, **16**(2014): 2958–2975. DOI: <https://doi.org/10.1039/C4GC00013G>.
- [17] J. Dobson. *Drug Dev. Res.*, **67**(2006):55–60. DOI: <https://doi.org/10.1002/ddr.20067>.
- [18] J. H. Lee, Y. M. Huh, Y. Jun, J. Seo, J. Jang, H. T. Song, S. Kim, E. J. Cho, H. G. Yoon, and J. S. Suh. *J. Cheon, Nat. Med.*, **13**(2007): 95–99. DOI: <https://doi.org/10.1038/nm1467>.
- [19] A. K. Gupta and M. Gupta. *Biomater.*, **26**(2005):3995–4021. DOI: <https://doi.org/10.1016/j.biomaterials.2004.10.012>.
- [20] A. H. Lu, W. Schmidt, N. Matoussevitch, H. Bpnnermann, B. Spliethoff, B. Tesche, E. Bill, W. Kiefer, and F. Schüth. *Angew. Chem.*, **116**(2004):4403–4406. DOI: <https://doi.org/10.1002/anie.200454222>.
- [21] W. Weiss and W. Ranke. *Prog. Surf. Sci.*, **70**(2002):1–151. DOI: [https://doi.org/10.1016/S0079-6816\(01\)00056-9](https://doi.org/10.1016/S0079-6816(01)00056-9).
- [22] M. Port A. Roch C. Robic L. Vander Elst R. N. Muller S. Laurent, D. Forge. *Chem. Rev.*, **108**(2008):2064–2110. DOI: <https://doi.org/10.1021/cr068445e>.
- [23] L. Z. Fekri, M. Nikpassand, and S. N. Khakshoor. *J. Orgmet. Chem.*, **894**(2019):18–27. DOI: <https://doi.org/10.1016/j.jorganchem.2019.05.004>.
- [24] A. R. Sardarian and I. Dindarloo Inaloo. *RSC Adv.*, **5**(2015):76626–76641. DOI: <https://doi.org/10.1039/C5RA14528G>.
- [25] A. R. Sardarian, I. Dindarloo Inaloo, A. R. Modarresi-Alam, E. Kleinpeter, and U. Schilde. *J. Org. Chem.*, **84**(2019):1748–1756. DOI: <https://doi.org/10.1021/acs.joc.8b02191>.
- [26] I. Dindarloo Inaloo and S. Majnooni. *Chemistry. Select*, **3**(2018): 4095–4100. DOI: <https://doi.org/10.1002/slct.201800107>.

- [27] M. Mokhtary. *J. Iran. Chem. Soc.*, **13**(2016):1827–1845.  
DOI: <https://doi.org/10.1007/s13738-016-0900-4>.
- [28] Sh. Vajar and M. Mokhtary. *Polycycl. Arom. Comp.*, **39**(2019):111–123.  
DOI: <https://doi.org/10.1080/10406638.2017.1280516>.
- [29] M. Foroughi Kaldareh, M. Mokhtary, and M. Nikpassand. **34**(2020):e5469.  
DOI: <https://doi.org/10.1002/aoc.5469>.
- [30] H. Dadhania, D. Raval, and A. Dadhania. *Polycycl. Arom. Comp.*, **41**(2021):440–453.  
DOI: <https://doi.org/10.1080/10406638.2019.1595057>.
- [31] D. Katheriya, N. Patel, H. Dadhania, and A. Dadhania. *J. Iran. Chem. Soc.*, **18**(2021):805–816.  
DOI: <https://doi.org/10.1007/s13738-020-02069-9>.
- [32] R. M. Vala and H. M. Patel. *Adv. Heterocycl. Chem.*, **141**(2023):179,  
DOI: <https://doi.org/10.1016/bs.aihch.2023.04.001>.
- [33] L. Z. Fekri and S. Zeinali. *Appl. Orgmet. Chem.*, **34**(2020):e5629.  
DOI: <https://doi.org/10.1002/aoc.5629>.
- [34] M. Nikpassand, A. Keyhani, L. Z. Fekri, and R. S. Varma. *J. Mol. Struct.*, **1251**(2022):132065, .  
DOI: <https://doi.org/10.1016/j.molstruc.2021.132065>.
- [35] M. Nikpassand, L. Zare Fekri, and P. Farokhian. *Synth. Commun.*, **45**(2015):2303–2310, .  
DOI: <https://doi.org/10.1080/00397911.2015.1077256>.
- [36] L. Zare Fekri and A. R. Darya-Laali. *Polycycl. Arom. Comp.*, **40**(2020):1539.  
DOI: <https://doi.org/10.1080/10406638.2018.1559207>.
- [37] A. M. Shahi, M. Nikpassand, and L. Z. Fekri. *Org. Prepare. Proc. Inter.*, **51**(2019):521–529.  
DOI: <https://doi.org/10.1080/00304948.2019.1666637>.
- [38] L. Z. Fekri, H. Hamidian, and M. A. Chekosarani. *RSC adv.*, **10**(2020):556–564, .  
DOI: <https://doi.org/10.1039/C9RA08649H>.
- [39] M. Mirhosseini, F. Nemati, and A. Elhampour. *J. Iran. Chem. Soc.*, **14**(2017):791–801.  
DOI: <https://doi.org/10.1007/s13738-016-1029-1>.
- [40] P. kamalzare, B. Mirza, and S. Soleimani-Amiri. *J. Nanostruct. Chem.*, **11**(2021):229–243.  
DOI: <https://doi.org/10.1007/s40097-020-00361-x>.
- [41] M. Nasr-Esfahani, S. Jafar Hoseini, M. Montazeezohori, R. Mehrabi, and H. Nasrabadi. *J. Mol. Catal.A: Chem.*, **382**(2014):99–105.  
DOI: <https://doi.org/10.1016/j.molcata.2013.11.010>.
- [42] M. Bakhtiarian and M. M. Khodaei. *Mater. Today Commun.*, **29**(2021):102791.  
DOI: <https://doi.org/10.1016/j.mtcomm.2021.102791>.
- [43] B. Maleki, H. Atharifar, O. Reiser, and R. Sabbaghzadeh. *Polycycl. Arom. Comp.*, **41**(2021):721–734.  
DOI: <https://doi.org/10.1080/10406638.2019.1614639>.